DESIGN OF A FATIGUE RIG FOR TESTING TURBINE BLADES UNDER CYCLING LOADING AT AMBIENT AND ELEVATED TEMPERATURE

Mélanie Leroy, Alain Köster, David Ryckelynck, Luc Rémy

Centre des Matériaux, Mines de Paris, Paristech, CNRS UMR 7633, BP 87, 91003 Evry Cedex, France

Abstract. During manufacturing of single crystal turbine blade, various foundry defects can occur. In service, presence of such defect could lead to blade failure. Indeed, gas turbine blades undergo severe and complex thermal loading conditions such as creep, fatigue, temperature gradients and localization of stress due to the complex geometry of the blade. The goal is to evaluate properly the influence of foundry defects, such as the presence of two grains in the turbine blade, on the blade lifetime. Snecma manufactures bi-crystal blades in order to evaluate the influence of the presence of grain boundary on the crack initiation.

1 INTRODUCTION

In service, gas turbine blades are subjected to high temperature, which require high strength, creep, oxidation and corrosion resistance. To be resistant on creep, single crystal turbine blades are formed using the directional solidification technique in order to have no grain boundary in the material. Combined to the crystal orientation, the mechanical properties are optimised to creep and fatigue at elevated temperature (>1000°C).

The insertion of a grain boundary as a defect inside a single crystal blade, which becomes a bi-crystal blade, can modify the lifetime like as instance the presence of a pore, which lead to a crack initiation [1].

The bi-crystal blade is constituted of two single crystals from the bottom to the top of the blade, the material is AM1 a superalloy nickel based. The two grains differ by their crystallographic orientation, inducing different mechanical behaviour [2]. The effect of such defect on the lifetime of a turbine blade has to be evaluated like other classical casting defects.

The presence of different crystallographic orientation can lead to the rupture of the blade during working due to the stress concentration at the interface of the two single crystals. Moreover the presence of a grain boundary can lead to a failure considering its favourable place for cracks initiation.

The foundry of Snecma supplied different bi-crystal blades with different crystallographic orientations. The position, shape and geometry of the grain boundary are considering as parameters for the lifetime of the blade. To solicit the grain boundary of the real turbine blades, a special assembly has to be designed for taking place on a servo-hydraulic testing machine, the heating system for tests at elevated temperature will be a induction heating

2 CONCEPTION OF A FATIGUE TEST RIG

The aim of the project is to test a real turbine blade instead of specimen, thus it is needed to design a fatigue rig adaptable on a fatigue machine in order to solicit the turbine blade. The tests will be performed at ambient temperature but also at elevated temperature (650°C and over) and different techniques of field measurement (mechanical and thermal) have been prepared to follow the displacement of the blade and the temperature gradient.

2.1 Design and validation of the fatigue rig

2.1.1 Conception of the rig to test real turbine blade

In order to test the real turbine blade, an assembly has been conceived using *Catia V5* software.

The fatigue rig allows the maintaining of the blade bottom by fitting perfectly the blade shape. The position of the load to be applied (figure 1) can be chosen by translating (lateral and horizontal) and rotating the blade. An additional part had been design in order to load the blade using a surface contact. Likewise, a part was designed to block the actuator in rotation. During the conception of the assembly, the possibility to introduce a heating induction for tests at elevated temperature has been taking into account.

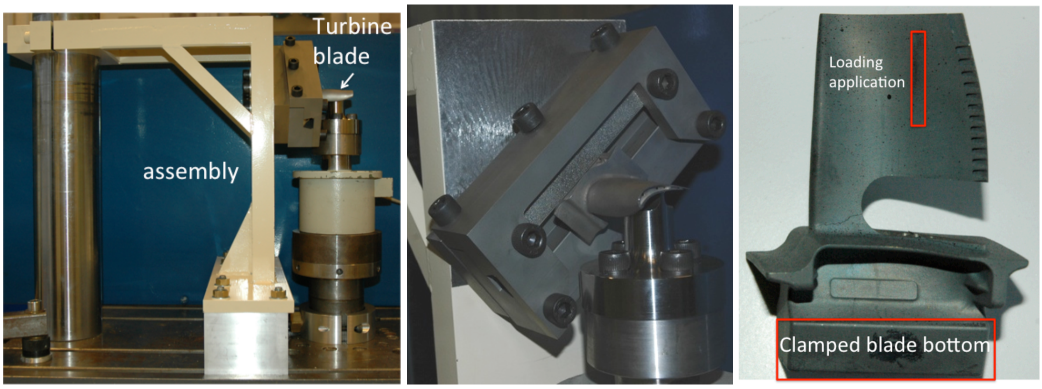

Figure 1: assembly and boundaries conditions for tested blades.

2.1.2 *Different techniques of field measure implementing during the test*

During the test, different observations techniques have been implementing:

- Displacement measurement by LVDT;
- Infrared thermography measurements.

The LVDT (Linear Variable Differential Transformer) allows following the punctual displacement (figure 2) on the blade placed at the bottom side extrados. For elevated temperature, the LVDT has been modified to protect it from the heat by using of an alumina stem between blade and LVDT.

The infrared thermography allows measurement of the thermal gradient during blade cycling and permits differed analysis.

Figure 2: position of the LVDT.

2.1.3 *Choice of the blades to be tested*

Snecma supplied several bi-crystal blades. These bi-crystal blades are uncoated and undergo heat treatments range to have the same mechanical behaviour as real single crystal blade in an engine aircraft.

Each blade is unique with interface geometry, an interface position and a crystallographic orientation, which are different from each other. For each blade, the orientation of each grain was checked by the Laue back-reflection X-ray technique and transformed in Euler angles to include the influence of crystallographic orientation in numerical simulations. The orientation of crystal in each grain is represented in Table 1, only three bi-crystal blades were chosen according to the position of the interface.

TURBINE BLADE	CRYSTALLOGRAPHIC ORIENTATION (°)		TESTS CONDITIONS	LIFETIME
	GRAIN1	GRAIN2		
Blade A 	φ_1: 18/ϕ: 9/φ_2: 78 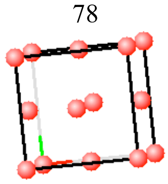	φ_1: 1/ϕ: 12/φ_2: 2 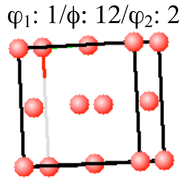	T (°C): 20 Freq. (Hz): 0,1 and 1 Load: 1,5kN Rε: 0,067	N: 109580

Blade B 	φ_1: 55/ϕ: 15/φ_2: 64 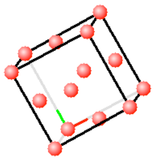	φ_1: 9/ϕ: 4/φ_2: 9 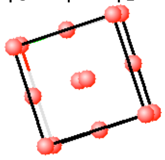	T (°C): 650 Freq. (Hz): 1 Load: 1,5kN Rε: 0,067 (20°C & 5 Hz for themography)	N: 768390
Blade C 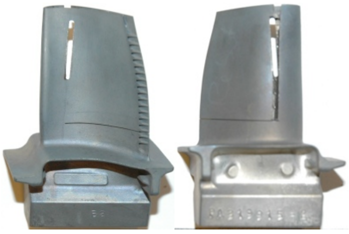	φ_1: 64/ϕ: 4/φ_2: 40 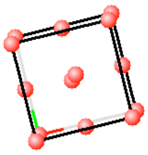	φ_1: 58/ϕ: 12/φ_2: 30 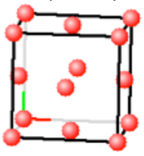	T (°C): 650 Freq. (Hz): 1 Load: 0,3kN Rε: 0,33	N: 243870

Table 1 – Tests conditions

2.2 Preliminaries simulations

Fatigue tests have been performed under cyclic loading. To prepare these tests, several numerical simulations are done to optimise the notch geometry and to determine the maximal load that could be applied on the blade. Fatigue tests are performed in elastic regime. The load value to satisfy the elastic return of the blade is determined by elasto-viscoplastic analysis [3].

The crystallographic orientation is taken into account in numerical simulation by the introduction of Euler angles in the definition of the material law. The evaluation of the number of cycle to attain the blade rupture is calculated by the criterion Fat-flu developed by ONERA.

3 TEST AT AMBIENT TEMPERATURE

A first test at ambient temperature has been done to validate the assembly. In service, turbine blades undergo elevated thermal gradient from 650°C (at the bottom) to 1100°C (at the top of the blade), but for the first test, it was easier to perform test and to do simulations at constant temperature. Moreover, field strain measurements at ambient temperature permit to validate simulations and experiments.

3.1 Modification of the blade geometry

The geometry of the blade is complex and involves stress concentration. In order to evaluate if the structure effect is uncorrelated of the grain boundary effect, the geometry of the blade has been changed (figure 3). A notch with a large diameter (12mm) was done. Notches are machining to maintain the grain boundary at the notch tip on both sides (intrados and extrados).

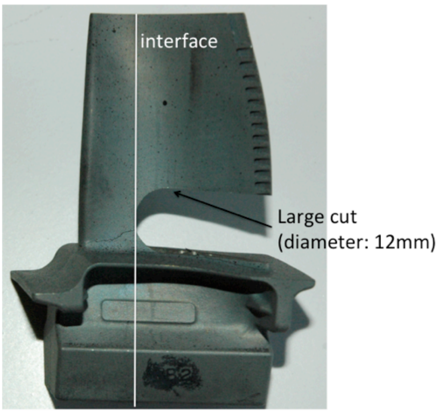

Figure 3: Modification of the blade geometry for blade A and B.

3.1.1 Material constitutive equations

In this work, the behavior of the nickel-based AM1, a FCC material, is described by a micro-macro model derived from slip theory developed by Méric [4]. Due to the cubic symmetry of the AM1, the total strain is split into two parts, elastic and plastic part

$$\underline{\varepsilon} = \underline{\varepsilon}^{e} + \underline{\varepsilon}^{p} \,, \underline{\sigma} = \underline{\underline{C}} : \varepsilon \tag{1), (2}$$

where $\underline{\underline{C}}$ is the elastic stiffness tensor. Plastic deformation is the result of activated slip systems composed by 12 octahedral slip systems and 6 cubic slip systems

$$\underline{\dot{\varepsilon}}^{p} = \sum_{s=1}^{12} \underline{m}^{s} \dot{\gamma}^{s} + \sum_{s'=1}^{6} \underline{m}^{s'} \dot{\gamma}^{s'} \text{ with } \underline{m}^{s} = \frac{1}{2}\left(\vec{l}^{\,s} \otimes \vec{n}^{s} + \vec{n}^{s} \otimes \vec{l}^{\,s}\right) \tag{3), (4}$$

where $\vec{l}^{\,s}$ is the slip direction and $\vec{\mathrm{n}}^{s}$ is the normal to the slip plane of each slip system.
The flow rule is

$$\dot{\gamma}^{s} = \left\langle \frac{\left|\tau^{s} - x^{s}\right| - r^{s}}{k} \right\rangle^{n} sign\left(\tau^{s} - x^{s}\right) \tag{5}$$

the isotropic hardening rule is given by

$$r^{s} = r_{0} + q \sum_{s} H^{sr}\left(1 - e^{-bv^{r}}\right) \text{ with } \dot{v}^{r} = \left|\dot{\gamma}^{r}\right| \tag{6}$$

and the non linear kinematic hardening rule is used

$$\dot{x}^{s} = c\dot{\gamma}^{s} - \dot{v}^{s} d x^{s} \tag{7}$$

3.2 Thermoelastic stress analysis

Thermography technique is using during test to have a rapid and noncontact imaging of the whole field of principal stresses, which can be recorded without any modification of the fatigue test procedure.

For the blade B, the infrared thermography technique has been used to locate the change of temperature due to the mechanical loading exerted on the blade at ambient temperature. At 650°C, the thermal gradient create a noise which disturb the thermoelastic stress analysis, no results were satisfactory.

Stress measurement of infrared thermography is possible for measuring a temperature evolution of blade by thermoelastic effect. The thermoelastic effect is to the thermodynamic relationship between the change of stress in a component under elastic loading and the corresponding change of temperature. It is simply proportional to the change in the sum of the principal stresses, if adiabatic conditions prevail.

The relationship between thermal stress and strain in an isotropic, elastic element is given by the thermodynamic equation

$$\Delta\varepsilon = \frac{(1-2v)\cdot\Delta\sigma}{E} + 3\alpha\Delta T \tag{8}$$

where $\Delta\varepsilon$ is the change in the sum of principal strains, $\Delta\sigma$ is the change in the sum of principal stresses (Pa), E is Young's modulus (Pa), v is Poisson's ratio, α is the coefficient of linear expansion (K^{-1}), ΔT is the change of temperature (K), $\Delta\varepsilon$ and $\Delta\sigma$ are invariants.

If the thermodynamic analysis is reversible, the behaviour of stressed is adiabatic and the specimen is elastic, the thermoelastic effect is described by this equation:

$$\Delta T = -\frac{\alpha}{\rho C_{p}} \cdot T \cdot \Delta\sigma \tag{9}$$

where ρ is the density ($kg.m^{-3}$), C_p the specific heat.

The assumption of thermoelastic stress analysis considers an adiabatic condition that is achieved by cyclic loading (>3Hz) of the stress structure. In this case a dynamic equilibrium (reversibility) is maintained between mechanical and thermal forms of energy.

Assumptions: emissivity non-constant because of the strong temperature gradient present in the blade (from 400 to 700°C). Under nonadiabatic conditions [5], heat diffusion attenuates the spatial temperature gradients, which leads to an underestimation of stress concentrations.

A cyclic loading of 5Hz was applied on the blade to perform stress analysis. Figure 4 represents the temperature analysis with the overheating area of the blade and the thermoelastic stress analysis corresponding to this overheating. Stress locales in the zone of the interface at the extrados. The comparison with numerical simulation shows the same zone of stress concentration at ambient temperature. Principal stresses are extracted from camera analysis and compared to Von Mises stresses from numerical simulation in figure 5.

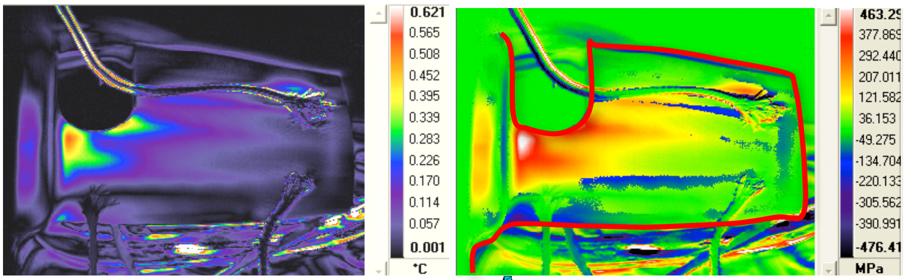

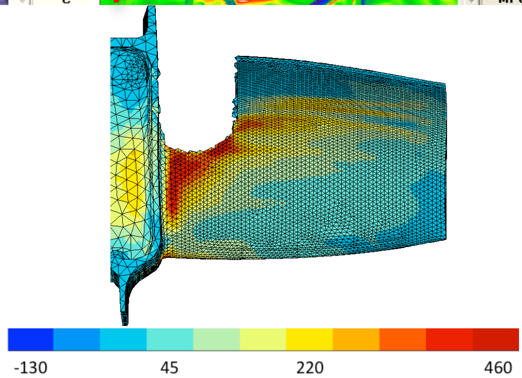

Figure 4: temperature analysis (right) and thermoelastic stress analysis (left).
Figure 5: Von Mises stress analysis [MPa] by numerical simulation

3.3 Test results

At ambient temperature, the crack initiation (figure 6) occurs near the platform, the weakest part of the blade. The crack follows different slip planes to liberate the energy in a minimum of time. The lifetime is indicated in table 1. For the numerical simulation (figure 7), elements were removed from the initial blade mesh to represent the same geometry modification as the tested blade. The localisation of cumulated octahedral slips show takes place at the same place than the crack initiation in tested blade.

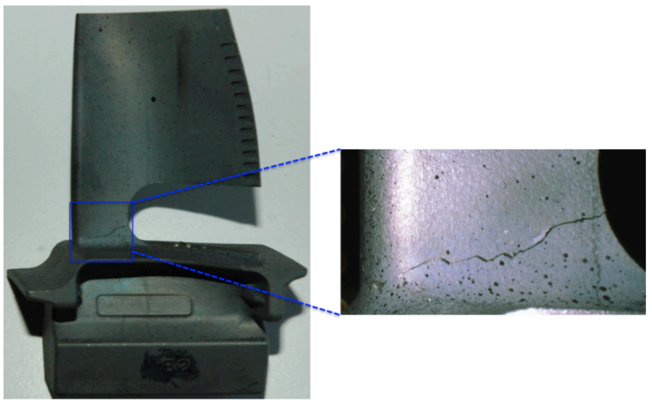

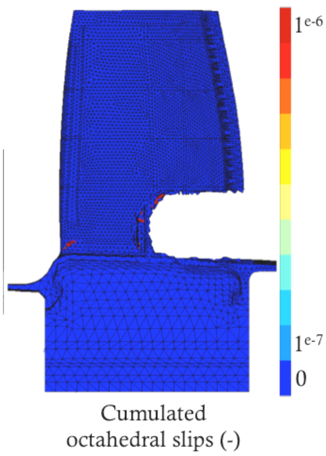

Figure 6: Crack propagation on blade A.
Figure 7: cumulated octahedral slip.

4 TESTS AT ELEVATED TEMPERATURE

Considering tests at elevated temperature, we choose a first temperature of 650°C to have apparition of slip systems according to the work of Hanriot [6,7]. Two tests were performed with different blade geometry modifications.

4.1 Conception of the induction heating

In order to heat the turbine blade to 650°C, an induction heating (figure 8) has been used and then an inductor was designed. In fact, the geometry of the rig does not allowed us to have a traditional heating system like with a LCF specimen. The geometry of the inductor is important: it should not heat the assembly but only the turbine blade. The geometry given to the copper tube is essential: the tube is twisted in order to reduce the value of the inductance.

This type of inductor doesn't give a uniform temperature in the blade but a temperature gradient (figure 9) from the platform to the top of the blade. A water-cooling system allows cooling the load cell and the part supporting on the blade. The temperature is included from 400° at the platform of the blade to 700°C at the top of the blade. The gradient induces a different mechanical behaviour inside the blade because of the Young's modulus dependency versus temperature. Higher the temperature is, smaller the young's modulus value is.

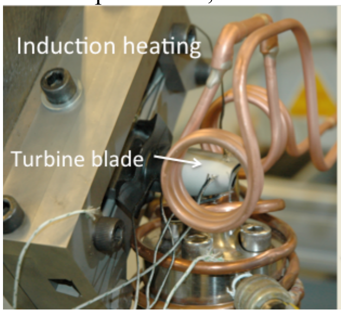

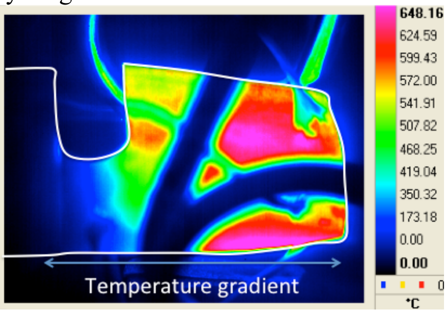

Figure 8: Induction heating.
Figure 9: Temperature gradient or thermal gradient

4.2 Comparison between the test at ambient temperature and the test at elevated temperature

For the two tests, cracks initiation occur in the same area but for the heated blade (figure 10), the initiation is slightly shifted to the top of the blade due to the evolution of Young's modulus with the temperature. Indeed, the temperature is increasing from the bottom to the top of the blade, which is accompanied by a significant reduction of Young's modulus.

Concerning cracks propagation, the crack path follows various activated slip planes (figure 12) with a irregular path because the behaviour of the AM1 is less viscous than at 950°C for example [8]. The interface seems to have no role for cracks initiation and propagation. The heated blade and the ambient blade haven't the same lifetime but we can't compare them because of the difference of frequency, of procedure (2 or 1 frequency per test) and at ambient temperature, crystallographic orientation effect is more influent than at elevated temperature.

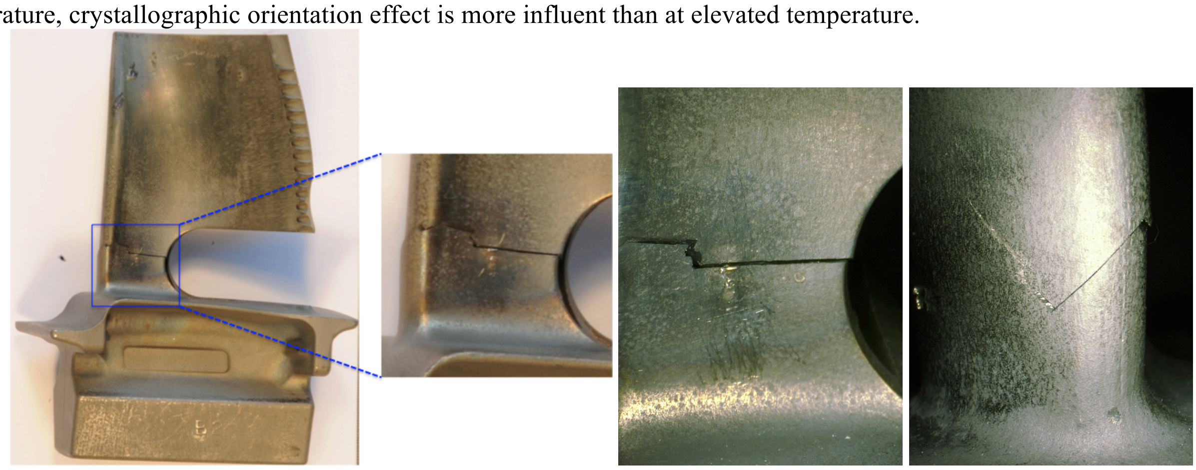

Figure 10: Crack propagation on blade B.

4.3 Modification of the blade geometry of PA319915-2

For the two precedent tests, the structure effect of the blade is more significant than the interface effect on the lifetime because of the type of loading and the chosen geometry modification. We would perform flexion test and the complex geometry of the blade prevent this opportunity. The blade geometry is constituted by two curved plates connect between them by reinforcements, which form the wall of cooling system. To have a part, which behave like a plate in flexion, the solution is to pull out a portion of the extrados (see Table 1), thus the intrados can be in flexion during loading.

4.4 Test results

The crack propagation is different compared to the previous tests. Indeed, in the two first tests, crack follows slip planes, so cracks are straight and the grains interface has no influence for crack initiation and propagation. For the last test, the crack is more tortuous and seems to follows grain boundary (figure 11). Complementary observations have to be done near the crack tip to confirm that the crack follows strictly or not the grain boundary. A touchy chemical attack is needed for revealing the grain boundary and allows the observation of both crack path and grain boundary. At this time, this work has not be done.

In numerical simulation (figure 12), elements were removed from the initial blade mesh to represent the same modification geometry as the tested blade. Simulation was done at a constant temperature of 650°C instead of a thermal gradient like in test to simplify the calculation. Simulation taking into account the gradient temperature will be performed with a refinement of the mesh.

In numerical simulation, plastic strain concentration (cumulated octahedral slips) and the Onera criterion show the same crack initiation zone.

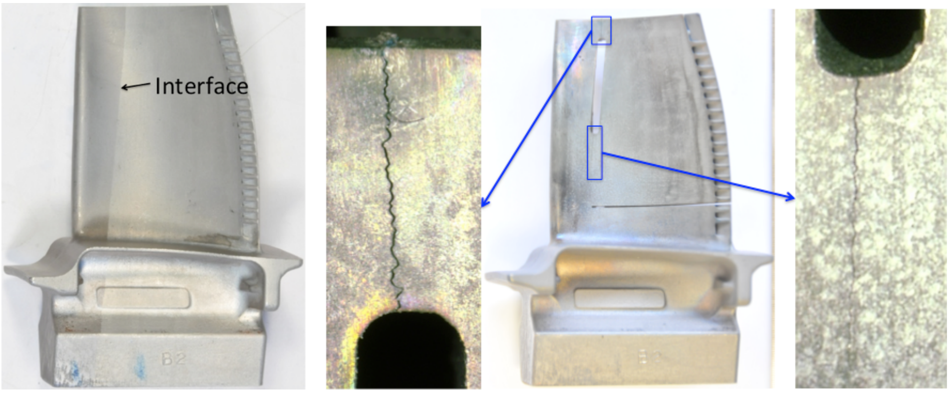

Figure 11: Crack propagation on PA319915-2

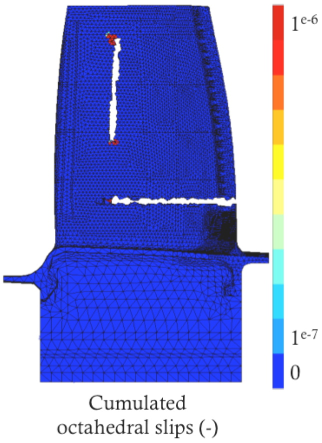

Figure 12: cumulated octahedral slip

5 CONCLUSIONS

The fatigue test rig has been conceived specially for testing real turbine blade and was validated by the first test. We were able to have a crack initiation and propagation during tests at ambient or elevated temperature with the fatigue test rig. The conception of the induction heating allows having a temperature gradient from 400°C to 650°C without heat the fatigue test rig.

The preliminary numerical simulations have predicted for each test where the crack initiation will take place. The role of the blade geometry is taken into account for the notch geometry and position to maximise the grain boundary loading. We succeed to have a blade rupture at elevated temperature at the grain boundary because of the choice of the notches localisation. The used of the criterion Fat-flu developed by ONERA allows to have an indication of the crack propagation place and of the number of cycle to have blade rupture.

The rupture of the blade but not at the grain boundary involves the activation of different slips systems and it will be interesting to determine which slip systems are activated versus the crystallographic orientation.

Complementary tests must be performed to observe the influence of crystallographic orientation on blade rupture and crack propagation and initiation

6 REFERENCES

1-M. Geuffrard, Amorçage et micro-propagation de fissure en fatigue à haute temperature à partir de défauts dans un superalliage monocristallin, PhD Thesis, Ecole Nationale Supérieure des Mines de Paris, 2010
2-R. V. Miner, R. C. Voigt, J. Gayda, T. P. Gabb, *Metall. Trans.*, 17 (A), 1986, 491-496
3-G. Cailletaud, plastOx,
4-L. Méric, P. Poubanne and G. Cailletaud, *Journal of Engineering Materials and Technology*, 133 (1), 1991, 162-170
5-S. Offermann, J. L. Beaudoin, C. Bissieux and H. Frick, *Experimental Mechanics*, 34 (4), 1997, 409-413
6-F. Hanriot, Comportement du superalliage monocristallin AM1 sous sollicitations cycliques, PhD Thesis, Ecole Nationale Supérieure des Mines de Paris, 1993, 18-33.
7-F. Hanriot, G. Cailletaud and L. Rémy, *The American Society of Mechanical Engineers*, 1991, 139-150
8-E. Fleury, Endommagement du superalliage monocristallin AM1 en fatigue isotherme et anisotherme, PhD Thesis, Ecole Nationale Supérieure des Mines de Paris, 1991